EAST EUROPEAN JOURNAL OF PHYSICS. 4. 48-56 (2022)
DOI:10.26565/2312-4334-2022-4-03 ISSN 2312-4334

ANALYSIS OF α-^{208}Pb ELASTIC SCATTERING IN A WIDE ENERGY RANGE BY THE *S*-MATRIX MODEL[†]

Yuri A. Berezhnoy[a‡], Gennadiy M. Onyshchenko[a], Volodymyr V. Pilipenko[b*], Pylyp E. Kuznietsov[a], Ivan I. Yakymenko[a]
[a]*V.N. Karazin Kharkiv National University, Kharkiv 61022, Ukraine*
[b]*National Science Center "Kharkiv Institute of Physics and Technology", Kharkiv 61108, Ukraine*
**Correspondence Author: vpilipenko@kipt.kharkov.ua; ‡E-mail: yuberezhnoy@karazin.ua*
Received August 31, 2022; revised October 5, 2022; accepted October 21, 2022

The paper analyzes the elastic scattering of α-particles on heavy ^{208}Pb nuclei at energies 26–175 MeV/nucleon using the original six-parameter *S*-matrix model, taking into account the strong absorption and pronounced effects of refraction of scattered waves. By fitting experimental data from the literature, measured in a wide range of energies: 104, 139, 166, 172, 240, 288, 340, 386, 480, and 699 MeV, the diffraction and refractive patterns of scattering have been investigated. The behavior of the found parameters of the model, as well as of the total reaction cross-section, the angles of crossover of the near and far components of the scattering amplitude (Fraunhofer intersection), and the angles of the nuclear rainbow have been studied and a comparison with the differential cross sections calculated according to the optical model is presented.
Keywords: Elastic Scattering; Scattering Matrix; ^{4}He+^{208}Pb; Nuclear Refraction; Nuclear Rainbow; Fraunhofer Crossover, Airy Minimum, Total Cross-Section
PACS: 25.55.Ci, 24.10.Ht

Investigation of hadron interaction with nuclei is an important source of information about the nuclear structure and mechanisms of the nuclear interaction. Approaches based on different potentials (optical model) or scattering matrix (*S*-matrix) are used for the theoretical description of appropriate experimental data.

In the intermediate energy region, it is possible to consider the nucleus (by analogy with optics) as a drop of liquid which strongly absorbs incident particles. The most common approach is the optical model of nuclear scattering, which uses the model complex potentials with an imaginary part describing the incident hadron absorption by nuclei. Such an approach demands to solving the Schrödinger equation numerically to calculate different scattering characteristics and analyze their physical properties.

An alternative approach is the analyzing of experimental data based on a model *S*-matrix specifically parametrized in the angular momentum or impact parameter space. In this case, it is often possible to obtain analytical expressions for the amplitudes and cross-sections of the analyzed processes, which makes it possible to study their dependence on different parameters of the *S*-matrix, and to understand deeper their physical meaning. Moreover, a reasonable parameterization of the *S*-matrix, containing a minimal number of parameters with a clear physical meaning, allows one to analyze experimental data in relatively wide ranges of energies and scattering angles, where different physical phenomena (Fraunhofer and Fresnel scattering, rainbow scattering etc.) are observed. In this case, certain difficulties of the optical model (uncertainty of the choice of parameters of the potential, non-Hermiticity of the Hamiltonian) are present. Besides, this approach allows one to understand certain features of the behavior of the differential cross-section of nuclear processes.

When 100–700 MeV alpha-particles are scattered on heavy nuclei, we obtain rapidly decreasing Fraunhofer oscillations of the elastic scattering differential cross-section in the region of small scattering angles. Further, we obtain a broad maximum, after which the cross-section decreases smoothly in the region of large scattering angles. Such a cross-section behavior is typically interpreted as a rainbow scattering [1-3]. However, while the energy of incident alpha-particles is increasing, the rainbow maximum becomes less pronounced, and the cross-section in the region of large angles is rapidly decreasing because it is determined by the far-side part of scattering amplitude, corresponding to the scattering from the far side of the target nucleus relative to the detector.

The rainbow scattering can be observed due to the little transparency of the target nucleus for the scattered light nuclei. In the case of rainbow scattering, the light incident particle comes into the inner region of the nucleus. Consequently, we obtain additional information about the inner nucleus structure by analyzing the differential cross-section. The rainbow scattering effect (which plays an essential role in nuclear collisions at intermediate energies) is also observed in the elastic scattering of ^{3}H, ^{3}He, ^{6}Li, ^{9}Be, ^{11}B, ^{12}C etc. by light and intermediate nuclei [2].

To find out the behavior of differential cross-section, it is necessary to determine the dependence of the quantum deflection function on the impact parameter or the angular momentum. If the deflection function has a deep minimum at negative values, it is possible to observe the nuclear rainbow scattering. Due to a small transparency in the scattering of some nuclei (^{9}Be, ^{12}C and others) one can observe only a faint hint of the rainbow scattering. This behavior of cross-section is called a rainbow ghost [1].

[†] ***Cite as:*** Yu.A. Berezhnoy, G.M. Onyshchenko, V.V. Pilipenko, P.E. Kuznietsov, and I.I. Yakymenko, East Eur. J. Phys. **4**, 48 (2022), https://doi.org/10.26565/2312-4334-2022-4-03
© Y.A. Berezhnoy, G.M. Onyshchenko, P.E. Kuznietsov, V.V. Pilipenko, I.I. Yakymenko, 2022

The picture of rainbow scattering in the region of intermediate energies ($E \geq 20$ MeV – 30 MeV/nucleon) for light and medium target nuclei and at somewhat higher energies for heavy nuclei is also determined by the combination of absorbing and refracting properties of the nuclear matter of the target with respect to the incident hadron and by the Coulomb interaction of colliding particles. Of particular interest is the cross-section behavior in the region of crossover of the near and far components of the scattering amplitude (Fraunhofer crossover) in a wide interval of energies for the elastic scattering of alpha particles on heavy nuclei.

This work analyzes and clarifies the regularities of elastic scattering of α-particles on heavy target nuclei (^{208}Pb) at energies up to 175 MeV/nucleon, inherent in the observed refraction phenomena. In this work, the diffraction and refraction phenomena in the scattering of α-particles on the heavy ^{208}Pb nucleus, as well as the interaction mechanisms of α-particles with these heavy nuclei, are investigated in the wide energy range from 104 to 699 MeV using of an original *S*-matrix model. The work is performed in the *S*-matrix approach, which was developed to describe the absorption and refraction effects in the elastic scattering of light nuclei at intermediate energies. We have obtained the scattering matrix parameters by fitting the experimental data on the elastic scattering of α-particles on the heavy ^{208}Pb nucleus for this *S*-matrix parameterization. We have determined the cross-section behavior in the region of crossover of the near and far components of the scattering amplitude (Fraunhofer crossover) and the angles of the nuclear rainbow in the wide interval of energies for the *α*–^{208}Pb elastic scattering.

To compare the fitting data quality, when using the above-mentioned model, we also present the results of analyzing the elastic scattering *α*–^{208}Pb at energies from 104 to 699 MeV by an alternative six-parameter optical model [4].

Based on the phenomenological S-matrix, we accurately describe the cross-sections of the elastic scattering *α*-^{208}Pb for the broad energy range of 104–699 MeV. This calculation results show the existence of strong nuclear refraction effects for the considered cases of elastic scattering, which can be interpreted as a "rainbow scattering".

The analysis identifies the nuclear rainbow effect in the differential cross-sections of elastic scattering ^{208}Pb(^{4}He, ^{4}He)^{208}Pb for E(^{4}He)= 104 [5], 139 [6], 166 [7], 172 [8], 240 [9], 288, 340 [10], 386 [11], 480, and 699 [10] MeV. The results show that the S-matrix parameters for the investigated cross-sections are sensitive to the interaction in the inner area of these heavy nuclei.

Besides investigating the nuclear rainbow for the elastic *α*–^{208}Pb scattering, we analyze the behavior of the Fraunhofer crossover angle and the nuclear rainbow angle depending on the energy value and the change in the shape of the quantum deflection function. It has been established that the Fraunhofer crossover angle θ_{cr} and the nuclear rainbow angle θ_r depend on the energy according to the exponential law as $\theta \sim \exp(-aE)$.

We also analyze the behavior of the nuclear refraction parameter δ_1 depending on the energy, which decreases exponentially, and nuclear transparency coefficient ε, which increases approximately linearly while the energy increases.

We investigate the behavior of critical radii $L_{0/1}/k$ and diffuseness parameters $\Delta_{0/1}/k$ of the strong absorption and nuclear refraction regions, which have an approximately linear dependence on the energy.

Therefore, the results indicate smooth, physically substantiated changes in the values of the parameters with a change in energy, which have a clear semiclassical interpretation.

1. *S*-MATRIX PARAMETERIZATION

In this work we use the following expression for the elastic scattering amplitude in terms of the *S*-matrix elements:

$$f(\theta) = \frac{1}{2ik}\sum_{l=0}^{\infty}(2l+1)\left[S_l - 1\right]P_l(\cos\theta)\,, \tag{1}$$

where θ is the scattering angle; l is the angular moment; k is the wave vector of the incident particle; S_l are the diagonal matrix element of the scattering operator in the representation of angular momentum, $P_l(\cos\theta)$ are the Legendre polynomials.

In doing so, we use the following original parametrization of the *S*-matrix as a function of the moment [1]:

$$S(L) = \exp\left\{-2\delta_a(L) + 2i[\delta_r(L) + \sigma_C(L)]\right\} = \eta(L)\exp\left\{2i[\delta_r(L) + \sigma_C(L)]\right\}, \tag{2}$$

$$\eta(L) = \exp\left[-2\delta_a(L)\right],\ \delta_a(L) = \delta_0\ g(L, L_0, \Delta_0)\,, \tag{3}$$

$$2\delta_r(L) = \delta_1\ g^2(L, L_1, \Delta_1)\,, \tag{4}$$

$$g(L, L_j, \Delta_j) = \frac{\mathrm{sh}(L_j/\Delta_j)}{\mathrm{ch}(L_j/\Delta_j) + \mathrm{ch}(L/\Delta_j)}, \qquad j = 0,1 \tag{5}$$

where $L = l + 1/2$ is an angular moment; $\eta(L)$ is the modulus of the scattering matrix; $\delta_a(L)$ is the nuclear imaginary phase shift due to the absorption; $\delta_r(L)$ and $\sigma_C(L)$ are the nuclear (refractive) and Coulomb phase shifts; $2\delta_0 = -\ln\varepsilon$ is the intensity of the nuclear absorption, $\varepsilon << 1$ being a parameter which defines the nuclear matter transparency for low moments; δ_1 is the parameter which characterizes the magnitude of nuclear refraction of the scattered waves; L_j and Δ_j

are the parameters which define the linear dimensions and diffuseness of the strong absorption ($j=0$) and nuclear reflection ($j=1$) regions.

The scattering phase $\delta_{\rm cl}$ in the quasi-classical approximation equals to:

$$\delta_{\rm cl}\left(L\right)=k\int\limits_{r_{\min}}^{\infty}\left[\left(1-\frac{U(r)}{E}-\frac{L^2}{k^2r^2}\right)^{1/2}-1\right]dr+\frac{\pi L}{2}-kr_{\min}\,, \tag{6}$$

where $r_{\min}$ is the classical distance of the closest approaching of the particle and nucleus, namely this quantity is defined from the equality to zero of the expression under the root in formula (6).

The potential energy of Coulomb interaction of the incident particle with the nucleus is chosen in the form of that for a uniformly charged sphere with the radius R_C :

$$U_C\left(R_C,r\right)=\begin{cases}\dfrac{Z_1Z_2e^2}{2{R_C}^3}\left[3{R_C}^2-r^2\right], & r<R_C\,,\\[2mm] \dfrac{Z_1Z_2e^2}{r}, & r\ge R_C\,,\end{cases} \tag{7}$$

Performing the integration in the expression (6) for the phase of scattering of a point-like charge on the potential of the uniformly charged sphere with the radius R_C (7) gives the quasi-classical expression for the Coulomb phase $\sigma_C(L)$ in the following explicit form [1]:

$$\sigma_C(L)=\begin{cases}-\dfrac{1}{2}\sqrt{L_C^2-L^2}-\dfrac{1}{4}p\ln\left[\dfrac{\left(aR_C^2-p+\sqrt{L_C^2-L^2}\right)^2}{p^2+L^2}\right]-n+\\[2mm] +n\ln\left(kR_C-n+\sqrt{L_C^2-L^2}\right)+L\left[\dfrac{1}{2}\,\mathrm{arctg}\,\dfrac{L^2+a\,p\,R_C^2}{L\sqrt{L_C^2-L^2}}+\right.\\[2mm] \left.+\,\mathrm{arctg}\left(L\,\dfrac{n\sqrt{L_C^2-L^2}-L^2-n\,k\,R_C}{L^2\sqrt{L_C^2-L^2}+nL^2+n^2kR_C}\right)+\dfrac{\pi}{4}\right], & L<L_C\,,\\[2mm] \dfrac{n}{2}\ln\left(L^2+n^2\right)+L\,\mathrm{arctg}\,\dfrac{n}{L}-n, & L\ge L_C\,,\end{cases} \tag{8}$$

where $L_C=(k^2R_C^2-2nkR_C)^{1/2}$; $k=\sqrt{2mE}/\hbar$; $a=(nk/R_C^3)^{1/2}$; $p=(3nk/R_C-k^2)/(2a)$; $n=\mu Z_1Z_2e^2/(\hbar^2k)$ is the Sommerfeld parameter; Z_1 and Z_2 are charge numbers of the incident particle and target nucleus; $\mu=(m_1m_2)/(m_1+m_2)$ is the reduced mass; for the scattering of *α*-particles one can take $R_C=1.3\sqrt[3]{A}$ fm, where *A* is the mass number of the target nucleus.

In the quasi-classical approximation, for particles approaching close to the nucleus boundary (grazing collisions), a boundary moment of strong absorption L_s is introduced. For the *S*-matrix model it is defined from the relation $\left|S(L_s)\right|=\eta(L_s)=(1+\varepsilon)/2$, where modulus $\eta(L)$ is defined from equation (3). Taking into account the deflection of incident particles in the Coulomb field, the quasi-classical boundary moment L_s is connected with the radius of strong absorption R_s by the relation:

$$L_s=kR_s\left[1-\frac{2n}{kR_s}+\frac{1}{(2kR_s)^2}\right]^{1/2}. \tag{9}$$

The radius R_s of the strong absorption region can be found from equality (9):

$$R_s=\frac{1}{k}\left[n+\left(L_s^2+n^2-\frac{1}{4}\right)^{1/2}\right]. \tag{10}$$

The formula (8) gives a good approximation if the condition $n/(L^2+n^2)<<1$ is satisfied (see [12]). In our calculations, in the $L\ge L_C$ region we use the exact expression for the Coulomb phase, which yields values very close to the corresponding values for $\sigma_C(L)$ from the quasi-classical expression (8).

The differential cross-section of elastic scattering is calculated as:

$$\sigma(\theta) \equiv \frac{d\sigma}{d\Omega} = \left| f(\theta) \right|^2 . \tag{11}$$

The quantum deflection function $\Theta(L)$ is related to the scattering phase $\delta(L) = \delta_r(L) + \sigma_C(L)$ by the formula:

$$\Theta(L) = 2\frac{d}{dL}\delta(L) . \tag{12}$$

The nuclear rainbow angle θ_r is defined as the depth of a minimum of the quantum deflection function (12). The nuclear rainbow effect is clearly observed only if the angle θ_r is substantially less than 180°. This condition is true if the energy of incident particle is not close to a specific critical energy $E_{\rm cr}$ (see [13]). For energies less than energy $E_{\rm cr}$, the rainbow structures in the cross-section are mainly observed for *α*-particle scattering on light and medium nuclei.

The search for the model parameters was carried out by obtaining the best agreement between the calculated elastic scattering cross section and the experimental data by minimizing the standard quantity χ^2. Experimental errors were normally taken to be 10% for all the data under consideration.

The formation of complex structures observed in the studied elastic scattering cross sections (for example, the Fraunhofer crossover) is analyzed using the decomposition of these cross-sections into near- and far-side components (see [1,14,15,16]).

2. RAINBOW EFFECTS IN THE ELASTIC SCATTERING OF *A*-PARTICLES ON ^{208}Pb NUCLEI IN THE ENERGY RANGE *E*=104 MeV–669 MeV

We present the results of the analysis of the available data on the elastic scattering of light ions ^{4}He on the ^{208}Pb nucleus in the energy range $E_α$ = 104–699 MeV, which is aimed at studying manifestations of the nuclear rainbow effect in this wide range of *α*-particle energies and determining the possibility of describing the differential cross-sections for ^{4}He scattering by heavy nuclei at intermediate energies using the *S*-matrix model, being an alternative to the optical model. We apply the 6-parameter model representation of the *S*-matrix [1], which was recently used for analyzing the ^{4}He scattering on light nuclei (^{12}C [2]) and ^{24}Mg [3]) and turned out to be successful in describing the nuclear rainbow picture of the ^{4}He scattering on these light nuclei at energies from 50 to 386 MeV. The *S*-matrix parameters for the investigated scattering cases have been obtained from analyzing the available experimental data (10 data sets) of the ^{4}He+^{208}Pb elastic scattering for energies 104 [5], 139 [6], 166 [7], 172 [8], 240 [9], 288, 340 [10], 386 [11], 480 and 699 [10] MeV.

The differential cross-sections of the *α*–^{208}Pb elastic scattering in the energy region $E_α$ = 104 MeV–669 MeV, calculated for the mentioned ten values of energy based on the *S*-matrix parametrization in the form (2) – (5), are given in Figs. 1-10. When calculating the scattering amplitude, the sum in formula (1) was taken for a wide range of *l* values to ensure sufficient accuracy of the calculated cross-sections. The *S*-matrix parameters were found by fitting to the corresponding experimental data [5–11], and further, their dependence on the energy was analyzed (Table). For comparison in Fig. 1-6, 8-10, we also present the differential cross-sections calculated basing on the 6-parameter optical model. In Table 1 the values of $\chi^2 / N_{\rm optic}$ are also given for them.

The considered cross-sections are characterized by pronounced refraction scattering pictures (see Figs. 1-10). In general, for the scattering of ^{4}He on this heavy nucleus a manifestation of the nuclear rainbow scattering is observed for all considered energies, according to the behavior of the deflection function. The deflection function $\Theta(L)$ has a shape which is characteristic of the nuclear rainbow, and it is symmetrical with respect to its minimum in the region of negative values.

With the energy increase, we note a gradual decrease of the magnitude of nuclear refraction intensity δ_1 and increase of the nuclear transparency ε (see Table, and Figs. 13,14 below).

Table. Energy evolution of the *S*-matrix parameters, the total reaction cross-section σ_r, the nuclear rainbow angle θ_r, the Fraunhofer crossover angle $\theta_{\rm cr}$, and the χ^2/N values for the calculated elastic scattering cross-sections.

$E_α$, MeV	k, fm^{-1}	L_0	L_0/k, fm	L_1	L_1/k, fm	Δ_0	Δ_0/k, fm	Δ_1	Δ_1/k, fm	ε	δ_1	*Lc*	χ^2/N, *S*-matr.	χ^2/N, optic.	σ_r, mb	θ_r, deg	$\theta_{\rm cr}$, deg
104	4.407	33.653	7.636	30.069	6.823	3.105	0.705	4.671	1.060	0.0022	32.871	28.484	4.3	9.7	3012.3	97.2	48.0
139	5.105	39.070	7.653	34.731	6.803	3.534	0.692	6.150	1.205	0.0025	35.400	34.712	6.0	-	2988.6	81.0	29.0
166	5.588	43.934	7.862	37.594	6.728	2.998	0.537	7.992	1.430	0.0217	28.906	38.869	7.1	16,1	2665.9	47.2	18.5
172	5.691	47.219	8.297	40.270	7.076	3.267	0.574	6.776	1.191	0.0280	23.220	39.737	0.9	-	2953.6	45.1	26.5
240	6.749	51.750	7.668	48.849	7.238	5.572	0.826	7.073	1.048	0.0114	18.205	48.572	6.3	-	3088.5	34.6	17.5
288	7.415	52.698	7.107	52.409	7.068	5.266	0.710	10.810	1.458	0.0018	20.801	54.014	4.9	4.9	2720.0	25.2	9.9
340	8.082	65.088	8.053	58.851	7.282	6.743	0.834	10.777	1.333	0.0510	16.250	59.408	4.9	5.8	3090.8	19.4	10.0
386	8.634	58.850	6.816	66.228	7.671	9.359	1.084	10.850	1.257	0.0088	10.158	63.848	4.3	-	3058.9	10.5	9.1
480	9.682	67.032	6.923	72.599	7.498	8.415	0.869	16.146	1.668	0.0240	10.902	72.198	9.9	8.6	2611.7	7.1	5.7
699	11.83	94.398	7.979	91.522	7.736	8.103	0.685	12.419	1.050	0.1508	4.222	89.167	2.0	6.2	2569.1	2.8	-

For the energy E_α= 139 MeV the nuclear rainbow effect is pronounced, and the differential cross-section in Fig. 2 has a noticeable "hump". At the energy E_α = 166 MeV, we observe two clear Airy minima (see Fig. 3).

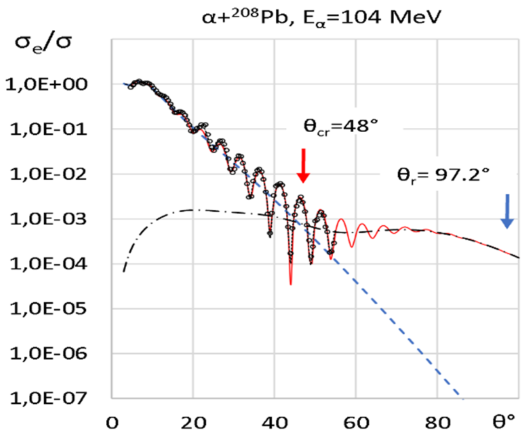

Figure 1. Differential cross-section (ratio to the Rutherford one) calculated with the *S*-matrix parametrization (2) – (5) and (8) for the elastic scattering α+^{208}Pb at E_α = 104.0 MeV (solid line), its far- (dot-dashed line) and near-side (dashed line) components, the dotted line is for the optical model. The experimental data are from [5]. Arrows show the rainbow and crossover angles.

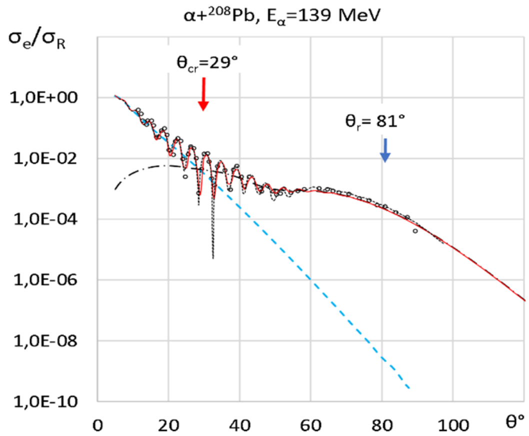

Figure 2. The same as in Fig. 1 but for E_α = 139.0 MeV (solid line), its far- (dot-dashed line) and near-side (dashed line) components, the dotted line is for the optical model. The experimental data are from [6].

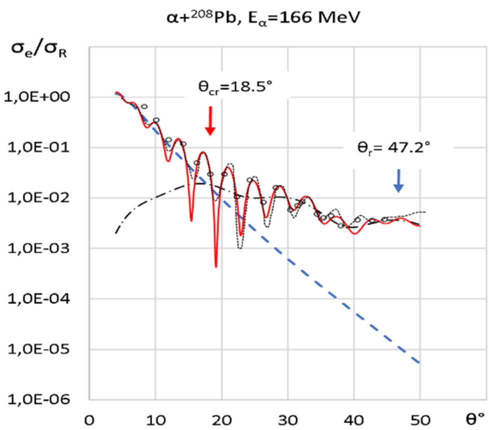

Figure 3. The same as in Fig. 1 but for E_α = 166.0 MeV (solid line), its far- (dot-dashed line) and near (dashed line) components, the dotted line is for the optical model. The experimental data are from [7].

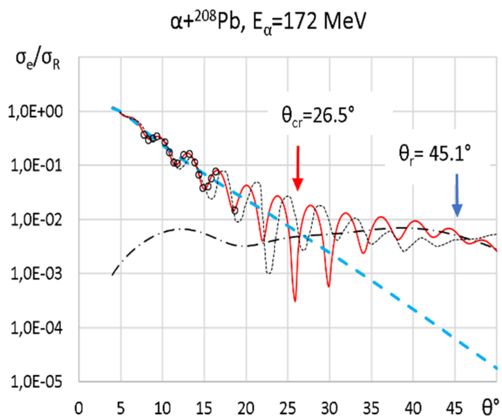

Figure 4. The same as in Fig. 1 but for E_α = 172.0 MeV (solid line), its far- (dot-dashed line) and near-side (dashed line) components, the dotted line is for the optical model. The experimental data are from [8].

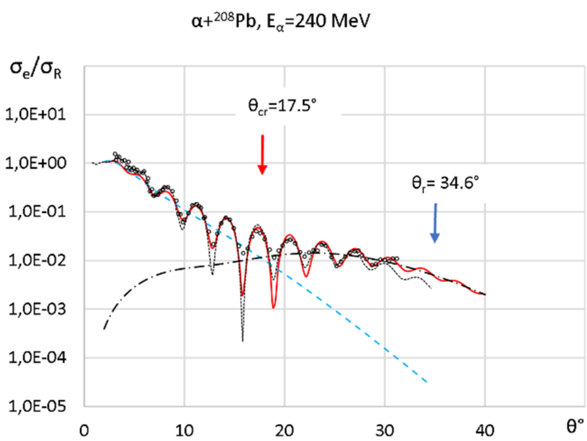

Figure 5. The same as in Fig. 1 but for E_α = 240.0 MeV (solid line), its far- (dot-dashed line) and near-side (dashed line) components, the dotted line is for the optical model. The experimental data are from [9].

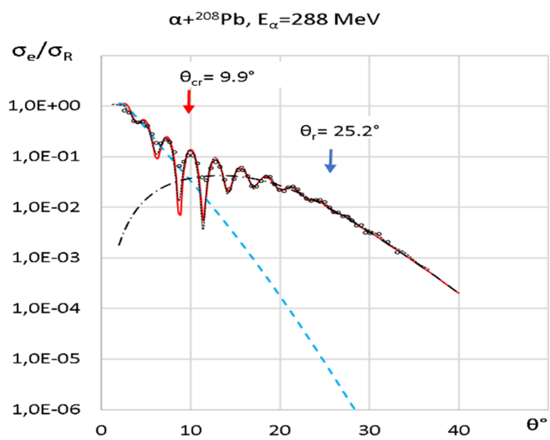

Figure 6. The same as in Fig. 1 but for E_α = 288.0 MeV (solid line), its far- (dot-dashed line) and near-side (dashed line) components, the dotted line is for the optical model. The experimental data are from [10].

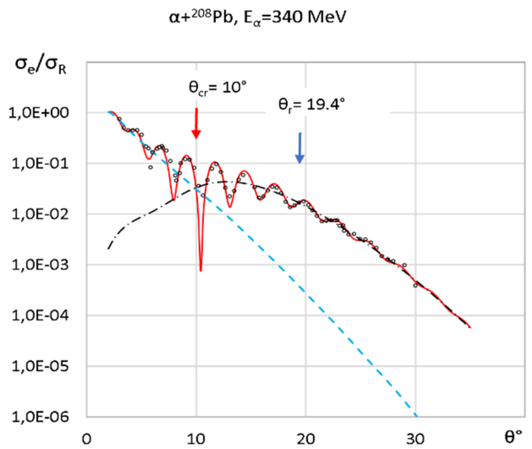

Figure 7. The same as in Fig. 1 but for $E_α$ = 340.0 MeV (solid line), its far- (dot-dashed line) and near-side (dashed line) components. The experimental data are from [10].

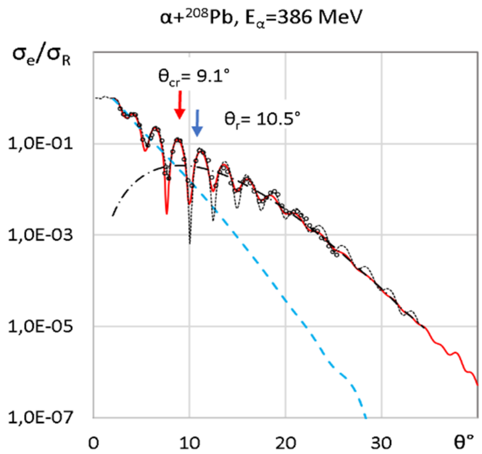

Figure 8. The same as in Fig. 1 but for $E_α$ = 386.0 MeV (solid line), its far- (dot-dashed line) and near-side (dashed line) components, the dotted line is for the optical model. The experimental data are from [11].

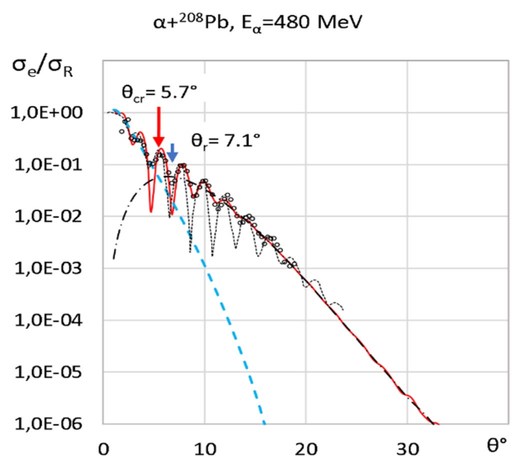

Figure 9. The same as in Fig. 1 but for $E_α$ = 480. 0 MeV (solid line), its far- (dot-dashed line) and near-side (dashed line) components, the dotted line is for the optical model. The experimental data are from [10].

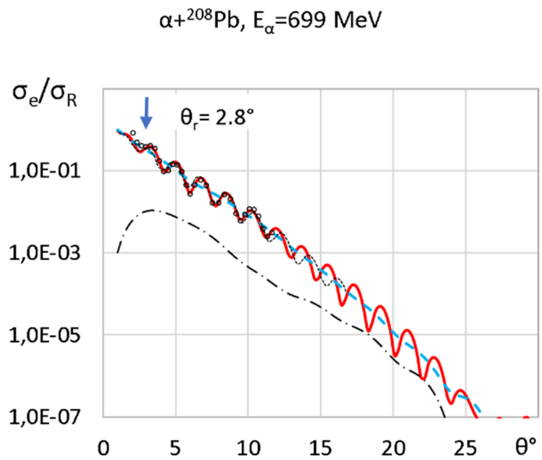

Figure 10. The same as in Fig. 1 but for $E_α$ = 699.0 MeV (solid line), its far- (dot-dashed line) and near-side (dashed line) components, the dotted line is for the optical model. The experimental data are from [10].

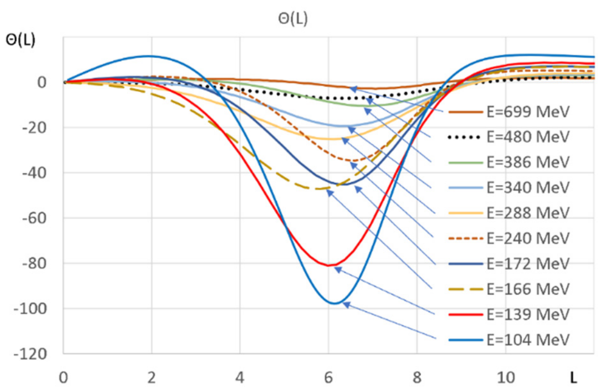

Figure 11. Quantum deflection function Θ(L) (degrees) as a function of angular momentum L for different energies.

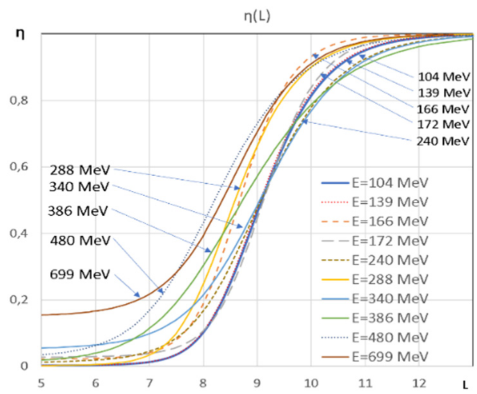

Figure 12. Dependence of the scattering matrix modulus $\eta(L)$ on the angular momentum L for different energies

Figures 1-10 show that the parameterization of the scattering matrix proposed by us makes it possible to correctly describe the complex behavior of the investigated differential cross-sections of elastic scattering of α-particles by heavy ^{208}Pb nuclei in wide ranges of energies and scattering angles. The experimentally measured cross-sections contain several periods of Fraunhofer oscillations in the region of small scattering angles, then the amplitude of the oscillations decreases and we observe a broad maximum, which is identified as the presence of rainbow scattering (nuclear rainbow).

Let us consider the behavior of the *S*-matrix as a function of the angular momentum *L* at different energies. Figures 11-12 demonstrate the behavior of the quantum deflection functions $\Theta(L)$ and the modulus $\eta(L)$ as functions of the angular momentum *L* for all considered cases of scattering for the α+^{208}Pb system. Figure 11 shows that the quantum deflection function $\Theta(L)$ has a deep minimum, which is typical for the nuclear rainbow. While the energy increases, the depth of the minimum of the deflection function $\Theta(L)$ (the rainbow angle) decreases substantially. Therefore, as can be seen from Figure 11 and Table, with the energy increase the nuclear rainbow angle θ_r decreases.

Figure 12 shows that the function $\eta(L)$ has the form of a "diffuse step", which changes rapidly at $L \approx L_0$, i.e. it demonstrates the effect of strong absorption *α*-particles by the lead nucleus at $L < L_0$.

The parameter δ_1, which characterizes the magnitude of the nuclear scattering phase, decreases with increasing energy (see Fig. 13) according to the law: $\delta_1 \sim \exp(-aE_\alpha)$, where a =0.03 MeV^{-1}.

The behavior of the nuclear matter transparency coefficient ε for the heavy ^{208}Pb nucleus with the energy increase is nearly linear (see Fig. 14), the variations are less than 5%, except for the last energy E_α = 699 MeV, where its increase up to 15% is observed.

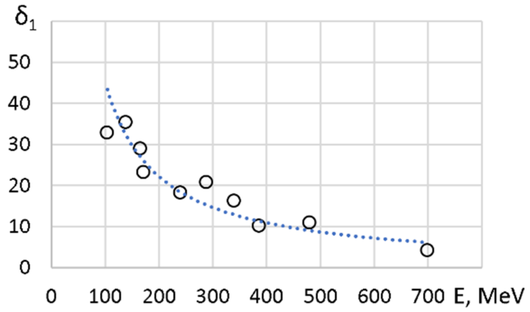

Figure 13. Parameter δ_1 characterizing the magnitude of the nuclear part of scattering phase (refraction coefficient), found on the basis of the *S*-matrix in the form (2) – (5) and (8) for the *α*+^{208}Pb elastic scattering, as a function of energy.

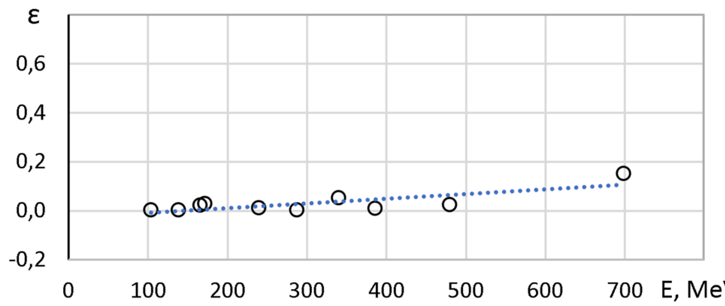

Figure 14. Nuclear matter transparency coefficient ε calculated basing on the *S*-matrix parametrization (2) – (5) and (8) for the α+^{208}Pb elastic scattering as a function of energy

Nuclear rainbow angle θ_r decreases with the energy increase (Fig. 15) and it may be approximated by the expression: $\theta_r \sim \exp(-aE_\alpha)$, where $a = 1.8$ MeV^{-1}. This is different from the dependence $\theta_r \sim 1/E$ proposed in [17].

The Fraunhofer crossover angle θ_{cr} decreases with the increasing energy (Fig. 16) and it may be approximated by the expression: $\theta_{cr} \sim \exp(-aE_\alpha)$, where $a = 1.3$ MeV^{-1}.

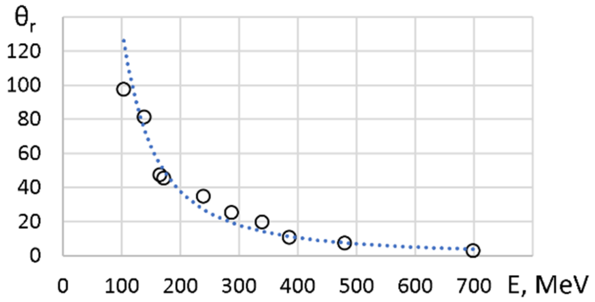

Figure 15. Nuclear rainbow angles θ_r, calculated basing on the *S*-matrix parametrization (2) – (5) and (8) for the *α*+^{208}Pb elastic scattering as a function of energy.

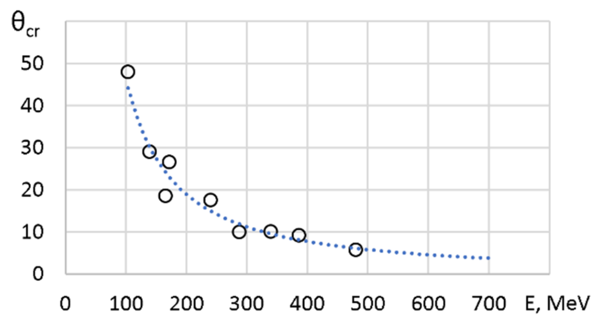

Figure 16. Fraunhofer crossover angles θ_{cr}, calculated basing on the *S*-matrix parametrization (2) – (5) and (8) for the *α*+^{208}Pb elastic scattering, as a function of energy.

The values of boundary radii L_0/k, L_1/k (fm) (Fig. 17) and diffuseness $d_0 = \Delta_0/k$, $d_1 = \Delta_1/k$ (fm) (Fig. 18) change slowly with increasing energy approximately according to a linear law.

Figure 19 shows that the total reaction cross-sections, calculated by the *S*-matrix model in the energy range 104-700 MeV practically do not change within a 10% error.

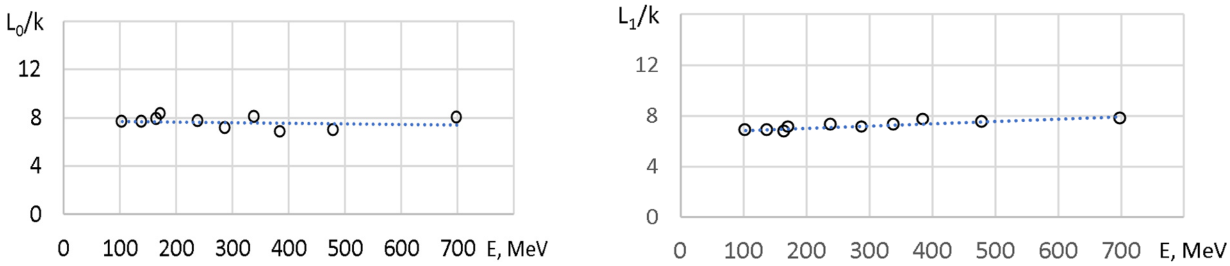

(a) (b)

Figure 17. Dependence of the boundary radii L_0 / k (a) and L_1 / k (b) (fm) on the energy.

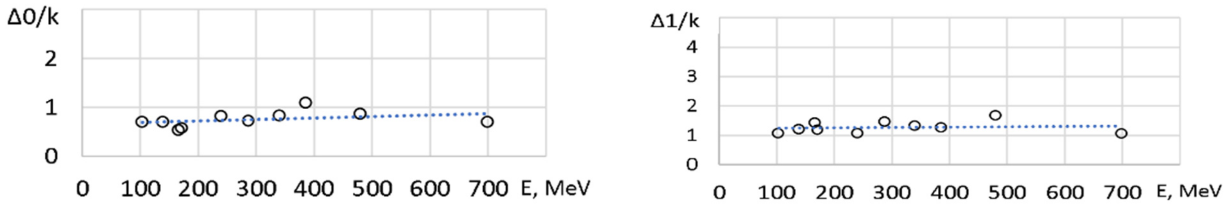

(a) (b)

Figure 18. Dependence of the diffuseness parameters Δ_0 / k (a) and Δ_1 / k (b) (fm) on the energy

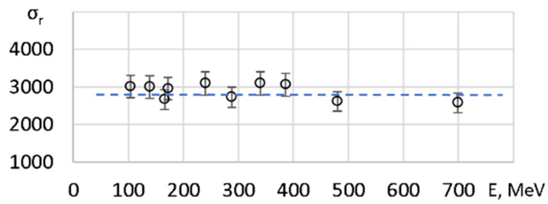

Figure 19. Total reaction cross-section σ_r (mb), calculated basing on the *S*-matrix parametrization (2)-(5) and (8) for the α+^{208}Pb elastic scattering, as a function of energy. The dashed line is drawn horizontally within 10% errors of the experimental data errors

CONCLUSION

The study of differential cross-sections of the elastic scattering of *α*-particles by heavy ^{208}Pb nuclei in the region of intermediate energies is a source of important information about mechanisms of nuclear interaction, as well as about the absorbing and refractive properties of the nuclear matter.

The completed analysis shows that the proposed six-parameter model of the scattering matrix successfully describes the differential cross-sections of the elastic scattering of *α*-particles by heavy ^{208}Pb nuclei in wide ranges of scattering angles (~5-90°) and energies (104-699 MeV) and explains the features of the nuclear rainbow effect in the elastic scattering without numerically solving the Schrödinger equation.

The obtained results of a correct systematic description of the *α*–^{208}Pb elastic scattering cross-sections for the in a wide energy range 104–699 MeV based on the phenomenological model representation of the scattering matrix indicate the presence of strong nuclear refraction in the considered scattering cases and lead to the “nuclear rainbow” interpretation of the analyzed data.

The nuclear rainbow effect has been identified in the differential cross-sections of elastic scattering of *α*-particles on the ^{208}Pb target nucleus for the energies E_α = 104, 139, 166, 172, 240, 288, 340, 386, 480, and 699 MeV, that is in the range of energies 26–175 MeV/nucleon. We have obtained the parameters of the scattering matrix by fitting the experimental data on the *α*–^{208}Pb elastic scattering on the basis of this original *S*-matrix approach and have studied the energy systematics of the nuclear rainbow angle and the angle of Fraunhofer crossover of near- and far-side components of the investigated angular distributions of cross-sections. The behavior of the shapes of the quantum deflection function and the modulus of the *S*-matrix depending on the energy has also been analyzed. The Fraunhofer crossover angle θ_{cr} and the nuclear rainbow angle θ_r, depending on the energy, behave as exp(-*aE*).

We have determined the tendencies of changing the absorbing (ε) and refractive (δ_1) properties of the nuclear matter with the energy change It has been established that the deflection function remains approximately symmetrical with respect to its minimum in the region of negative values with increasing energy.

The total reaction cross-sections σ_r, calculated on the basis of the parametrized *S*-matrix in the energy range 100–700 MeV, taking into account the experimental error of 10%, remain practically unchanged within these data errors.

We can note that with the energy increase the intensity of nuclear refraction δ_1 decreases approximately as $\exp(-aE_\alpha)$, and the nuclear transparency ε increases linearly. The boundary radii $L_{0,1} / k$ and diffuseness parameters

$\Delta_{0,1}/k$ for the strong absorption and nuclear refraction regions have a linear energy dependence. This indicates smooth, physically substantiated changes in the values of the parameters with a change in en7777ergy, which have a clear semiclassical interpretation.

A comparative analysis of the fit quality in the *S*-matrix and optical-model approaches shows a high quality of the fitting performed with the proposed six-parameter *S*-matrix model.

The results of the analysis show that the applied *S*-matrix approach may be used for further analyzing a wide variety of refraction phenomena, which are observed in the light-ion elastic scattering processes with heavy target nuclei, and for obtaining information about the interaction between nuclei and the nuclear structure from this analysis, as well as for determining the concrete ratio between the intensities of nuclear absorption, nuclear refraction and Coulomb interaction for investigated nuclear processes.

The investigation results allow the selection of unique nuclear systems and conditions to measure cross-sections of such nuclear processes, which may be sensitive to the studied effect.

ORCID IDs
Yuri Berezhnoy, https://orcid.org/0000-0002-9192-4801; **Gennadiy Onyshchenko**, https://orcid.org/0000-0001-6945-8413
Pylyp Kuznietsov, https://orcid.org/0000-0001-8477-1395; **Ivan Yakymenko**, https://orcid.org/0000-0002-0194-8376

REFERENCES

[1] Yu.A. Berezhnoy, and V.V. Pilipenko, "Analysis of refraction effects in nuclear scattering on the basis of the *S*–matrix approach", Mod. Phys. Lett. A, **10**(3), 2305 (1995). https://doi.org/10.1142/S0217732395002465
[2] Yu.A. Berezhnoy, G.M. Onyshchenko, and V.V. Pilipenko, "Analysis of α–^{12}C elastic scattering at intermediate energies by the *S*-matrix model", Int. J. Mod. Phys. E, **26**(5), 1750027 (2017). https://doi.org/10.1142/S0218301317500276
[3] Yu.A. Berezhnoy, A.S. Molev, G.M. Onyshchenko, and V.V. Pilipenko, "Unified *S*-matrix analysis of Airy structures in α+^{24}Mg elastic and inelastic scattering", Int. J. Mod. Phys. E, 27(7), 18500611 (2018). https://doi.org/10.1142/S0218301318500611
[4] P. Hodgson, *The Nucleon Optical Model*, (World Scientific, 1994). pp. 423.
[5] G. Hauser, R. Löhken, H. Rebel, G. Schatz, W. Schweimer, and J. Specht, "Elastic scattering of 104 MeV alpha particles", Phys. Lett. B, **27**, 220 (1968). https://doi.org/10.1016/0370-2693(68)90277-3
[6] D.A. Goldberg, S.M. Smith, H.G. Pugh, P.G. Roos, and N.S. Wall, "Scattering of 139-MeV Alpha Particles by 58Ni and 208Pb", Phys. Rev. C, **7**, 1938 (1973). https://doi.org/10.1103/PhysRevC.7.1938
[7] B. Tatischeff, and I. Brissaud, "166-MeV Elastic and Inelastic Alpha-Particle Scattering Macroscopic And Microscopic Analysis", Nucl. Phys. A, **155**, 89 (1970). https://doi.org/10.1016/0375-9474(70)90080-1
[8] H.P. Morsch, C. Sükösd, M. Rogge, P. Turek, H. Machner, and C. Mayer-Böricke, "Giant monopole and quadrupole resonances and other multipole excitations in 208Pb studied in 43 MeV/nucleon α-particle and deuteron scattering". Phys. Rev. C, **22**, 489 (1980). https://doi.org/10.1103/PhysRevC.22.489
[9] Do Cong Cuong, Dao T. Khoa, and Gianluca Colò, "Microscopic study of the isoscalar giant resonances in 208Pb induced by inelastic α scattering", Nuclear Physics A, **836**, 11 (2010). https://doi.org/10.1016/j.nuclphysa.2009.12.009
[10] B. Bonin, N. Alamanos, B. Berthier, G. Bruge, H. Faraggi, J.C. Lugol, W. Mittig, L. Papineau, A.I. Yavin, J. Arvieux, L. Farvacque, M. Buenerd, and W. Bauhoff, "Alpha-nucleus elastic scattering at intermediate energies", Nuclear Physics A, **445**(3), nj-407 (1985). https://doi.org/10.1016/0375-9474(85)90448-8
[11] M. Uchida, H. Sakaguchi, M. Itoh et.al, "Systematics of the bimodal isoscalar giant dipole resonance", Phys. Rev. C, **69**, 051301-1 (2004). https://doi.org/10.1103/PhysRevC.69.051301
[12] S.K. Kauffmann, "Refractive damping of Fraunhofer diffraction in light ion-nucleus elastic scattering at high energy", Z. Phys. A, **282**(2), 163 (1977). https://doi.org/10.1007/BF01408160
[13] K.W. McVoy, "Regge poles and strong absorption in heavy-ion and α-nucleus scattering", Phys. Rev. C, **3**(3), 1104 (1971).
[14] R.C. Fuller, "Qualitative behavior of heavy-ion elastic scattering angular distributions", Phys. Rev. C, **12**, 1561 (1975). https://doi.org/10.1103/PhysRevC.12.1561
[15] D.R. Dean, and N. Rowley, "Nearside-farside analysis of inelastic heavy-ion scattering", J. Phys. G, **10**(4), 493 (1984). https://doi.org/10.1088/0305-4616/10/4/011
[16] R.C. Johnson, "Spin-dependent interactions in nuclear reactions", J. Phys. Soc. Jpn. (Suppl), **55**, 7 (1986).
[17] J. Knoll, and R. Schaeffer, "Semiclassical scattering theory with complex trajectories. I. Elastic waves", Ann. Phys, **97**(2), 307 (1976). https://doi.org/10.1016/0003-4916(76)90040-3

АНАЛІЗ ПРУЖНОГО α-^{208}Pb РОЗСІЯННЯ В ШИРОКОМУ ІНТЕРВАЛІ ЕНЕРГІЙ ЗА *S*-МАТРИЧНОЮ МОДЕЛЛЮ

Ю. А. Бережной[a], Г. М. Онищенко[a], В. В. Пилипенко[b], П. Е. Кузнєцов[a], І. І. Якименко[a]
Харківський національний університет імені В.Н. Каразіна, 61022, Харків, Україна,
Національний науковий центр «Харківський фізико-технічний інститут», 61108, Харків, Україна

У роботі досліджено пружне розсіяння α-частинок на важких ядрах ^{208}Pb при енергіях 26-175 МеВ/нуклон з використанням оригінальної шести-параметричної S-матричної моделі, що враховує сильне поглинання і виражені ефекти заломлення розсіяних хвиль. За допомогою фітінгу експериментальних даних з літератури, виміряних в широкому діапазоні енергій: 104, 139, 166, 172, 240, 288, 340, 386, 480 і 699 МеВ досліджені дифракційні та заломлювальні картини розсіяння. Представлено поведінку знайдених параметрів моделі, а також повного перерізу реакції, кути перетину ближньої та дальньої складових амплітуди розсіювання (фраунгоферів перетин), кути ядерної райдуги, а також наведено порівняння з диференціальними перерізами, розрахованими за оптичною моделлю.

Ключові слова: пружне розсіювання; матриця розсіювання; 4he+208pb; ядерна рефракція; ядерна веселка; кросовер Фраунгофера, мінімум Ейрі, загальний поперечний переріз